SLAC–PUB–5128
LBL–27924
November, 1989
(T/E)

RADIATIVE TAU PRODUCTION AND DECAY †

D. Y. Wu,[a] K. Hayes,[b] M. L. Perl, G. S. Abrams, D. Amidei,[c] A. R. Baden,[d] T. Barklow, A. M. Boyarski, J. Boyer,[e] P. R. Burchat,[f] D. L. Burke, F. Butler,[g] J. M. Dorfan, G. J. Feldman, G. Gidal, L. Gladney,[h] M. S. Gold, G. Goldhaber, L. J. Golding,[i] J. Haggerty,[j] G. Hanson,[k] D. Herrup,[c] T. Himel, R. J. Hollebeek,[h] W. R. Innes, J. A. Jaros, I. Juricic,[e] J. A. Kadyk, D. Karlen,[l] S. R. Klein,[m] A. J. Lankford, R. R. Larsen, B. W. LeClaire,[n] M. E. Levi, N. S. Lockyer,[h] V. Lüth, M. E. Nelson,[a] R. A. Ong,[o] B. Richter, K. Riles,[p] P. C. Rowson,[e] T. Schaad, H. Schellman,[c] W. B. Schmidke, P. D. Sheldon,[q] G. H. Trilling, D. R. Wood,[r] and J. M. Yelton[s]

Lawrence Berkeley Laboratory and Department of Physics
University of California, Berkeley, California 94720

Stanford Linear Accelerator Center
Stanford University, Stanford, California 94305

Department of Physics
Harvard University, Cambridge, Massachusetts 02138

---

† This work was supported in part by the Department of Energy, contracts DE–AC03–76SF00515, DE–AC02–76ER03064, and DE–AC03–76SF–00098.

[a] Present address: California Institute of Technology, Pasadena, CA 91125
[b] Present address: Hillsdale College, Hillsdale, MI 49242
[c] Present address: Fermi Lab, Batavia, IL 60510
[d] Present address: University of Maryland, College Park, MD 20742
[e] Present address: Columbia University, NY, NY 10027
[f] Present address: University of California, Santa Cruz, CA 95064
[g] Present address: University of Oklahoma, Norman, OK 73019
[h] Present address: University of Pennsylvania, Philadelphia, PA 19104
[i] Present address: Therma-Wave Corp., Fremont, CA 94539
[j] Present address: Brookhaven National Laboratory, Upton, NY 11973
[k] Present address: Indiana University, Bloomington, Indiana 47405
[l] Present address: Carleton University, Ottawa, Ontario, Canada, K1S 5B6
[m] Present address: Boston University, Boston, MA 02215
[n] Present address: University of Wisconsin, Madison, WI 53706
[o] Present address: University of Chicago, Chicago, IL 60637
[p] Present address: University of California, Riverside, 92521
[q] Present address: University of Illinois, Urbana, IL 61801
[r] Present address: CERN, CH–1211 Geneva 23, Switzerland
[s] Present address: University of Florida, Gainesville, FL 32611

ABSTRACT

We have studied the muon decay channel of the τ lepton with the presence of a photon in e^+e^- annihilation data at E_{cm} = 29 GeV from the Mark II detector. Included in this study is the first direct measurement of radiative tau decay. We find the ratio of the measured $\tau \rightarrow \mu\gamma\nu\bar{\nu}$ branching fraction to the expected value from QED to be 1.03 ± 0.44.

Submitted to *Physical Review Letters*

A study of the muon decay channel of the τ lepton with the presence of a photon has been carried out to verify theoretical predictions for the production rate of $e^+e^- \rightarrow \tau^+\tau^-\gamma$ and for the branching ratio of $\tau \rightarrow \mu\gamma\nu\bar{\nu}$. This is the first direct measurement of radiative τ decay,[1] which for the muon channel with a detectable photon is expected to occur at the level of a percent of the total decay rate to $\mu\nu\bar{\nu}$. We are motivated by the one-prong τ decay branching ratio discrepancy[2–4] to check for anomalous behavior manifesting itself in radiative events.

We use e^+e^- annihilation data taken at $\sqrt{s}$=29 GeV with the Mark II detector at PEP[5,6] with an integrated luminosity of 207.9 pb^{-1}. The detector elements relevant to this analysis are briefly described here. There are two cylindrical drift chambers concentric with the beam direction which have combined momentum resolution of $\delta p/p = [(.025)^2 + (.01p)^2]^{1/2}$ (p in GeV/c) in the plane transverse to the beam direction. Surrounding the drift chamber is the Time-of-Flight(TOF) system, consisting of 48 plastic scintillators. Photons are detected by a barrel lead-liquid argon electromagnetic calorimeter, having an energy resolution of $\delta E/E \approx .14/\sqrt{E}$ (E in GeV)and covering 69% of the polar angle. There are also two endcap calorimeters with an energy resolution of $\delta E/E \approx .5/\sqrt{E}$ (E in GeV), which are used in this analysis for vetoing certain types of events. A muon detector surrounds the barrel calorimeter and consists of four walls, each with four layers of steel absorber and proportional tubes. This system covers $\sim$ 45% of the solid angle and limits our event acceptance. The Small Angle Tagger(SAT) detector resides at low forward angles with three sets of planar drift chambers, followed by plastic scintillators and a lead-scintillator calorimeter with energy resolution of $\delta E/E \approx .14/\sqrt{E}$ (E in GeV).[7]

Tau pairs in high energy e^+e^- experiments are generally produced collinearly unless hard initial-state radiation is emitted. They are detected by their decay products which emerge well collimated along the original τ direction and which usually include one to three visible charged tracks. Final-state radiation and decay radiation do not significantly alter the event topology. This analysis selects τ's which decay to a muon. In addition, one photon is required to be detected near the muon. In order to maintain high detection efficiency, we let the other τ decay to any mode, including the muon mode. Missing energy due to undetected neutrinos in τ events allows kinematic discrimination against radiative μ-pair events. Candidate events must pass the following criteria:[8]

- Two to six charged tracks, each with drift chamber momentum(p) $>$ .15 GeV.
- At least one charged track with p $\geq$ 2 GeV must have signals associated with it in all four layers of the muon system. This muon candidate must be isolated from other charged tracks by $> 90°$, a requirement which naturally divides the event into two hemispheres.
- Track quality cuts based on number of drift chamber hits, quality of the track fit, and distance of closest approach to the beam collision point must be satisfied. At least 2 tracks in a $<$ 4-charged track event and at least 3 tracks in a $\geq$ 4-charged track event must satisfy these cuts.
- Only one photon reconstructed in the barrel calorimeter with energy $\geq$ 0.3 GeV is allowed within 90° of the muon candidate.

The detection efficiency for .3 GeV photons is $\sim$ 72% and for $>$ .5 GeV photons, it is $>$ 95%.[9] For our muon definition, the detection efficiency for 2 GeV muons is $\sim$ 73% and for $>$ 4 GeV muons, it is $>$ 80%. From Monte Carlo τ pair events, where only one τ decays to the muon mode, we find the sole requirement of detecting a muon with p $\geq$ 2 GeV to have an efficiency of $\sim$ 21%. Expected backgrounds include radiative two-photon, radiative μ-pair and misidentified hadronic tau decay events. Backgrounds from multihadronic events, cosmic rays and events with spurious photons due to electronic noise are much smaller. Requiring the presence of a detected photon in the event significantly suppresses two-photon backgrounds. We further reject them by requiring the energy balance along the beam to satisfy:

$$\frac{|\sum_i p_{z_i}|}{|\sum_i \bar{p_i}|} \quad < \quad 0.92$$

where the summation is over charged and neutral tracks. We have requirements on the total energy(E_{VIS}) and the transverse momentum($P_\perp$) for the event, which include contributions from both charged and neutral particles. For events with > 2-charged tracks, we require $E_{VIS} > 6$ GeV. For 2-charged track events, we require $E_{VIS} >$ 3 GeV, and if $P_{\perp} < 3.5$ GeV then $E_{VIS} > 6.5$ GeV. Radiative μ-pair events are suppressed by demanding the following for 2-charged track events: E_{VIS} to be < 24 GeV, the event kinematics to be inconsistent with $e^+e^- \to \mu^+\mu^-\gamma$ hypothesis, and the acoplanarity to be > .25° (> 1° if both tracks are consistent with being muons). The acoplanarity is the acollinearity, in the plane transverse to the beam direction, of the total momentum of the charged track plus nearby photons in each hemisphere. There are also backgrounds from higher order radiative μ-pair events, characterized by missing energy from hard initial-state radiation close to the beam direction. These events are almost completely eliminated by requiring the missing mass, reconstructed from visible tracks, to be inconsistent with a photon mass, and the kinematic fit to be inconsistent with $e^+e^- \to \mu^+\mu^-\gamma(\gamma)_{beam}$ hypothesis. Because two-photon and hard-initial-state radiative processes sometimes emit electrons/positrons and photons at low angles, we veto events with total endcap-calorimeter energy > 8 GeV or with SAT system track energy > 3.5 GeV. Hadronic backgrounds are very small because of the required isolation of the muon candidate from other charged tracks. We discard events with > 2-charged tracks in the non-muon hemisphere, having a reconstructed mass > 2.5 GeV/c^2. Cosmic-ray events are removed by imposing a TOF cut on the difference between the expected and measured time for both tracks in all 2-charged-track events. Sixty-seven events survive all the above requirements.

Estimates of background contributions and selection efficiencies are calculated using the data and Monte Carlo techniques. For simulating τ-pair production, we use the Monte Carlo, KORALB,[10] which includes O(α) initial and final state radiative corrections and does not neglect the τ mass. To simulate multihadronic decays not in KORALB, we use the LULEPT [11] Monte Carlo program. We have modified the KORALB program to include the radiative decay, $\tau \to \mu\gamma\nu\bar{\nu}$, using formulas originally calculated for the process $\mu \to e\gamma\nu\bar{\nu}$, where lepton masses have not been neglected.[12,13] From the Monte Carlo $\tau \to \mu\gamma\nu\bar{\nu}$ events, generated with a minimum photon energy of .012 GeV in the τ rest frame, we find the probability for detecting a photon defined above, after the detection of a muon, to be $\sim 33\%$. For calculating expected backgrounds due to hadrons misidentified as muons, both from τ-pair events and from hadronic events, we measure the total probability of pion decay to muons plus misidentification from punchthrough using 1054 pion tracks from $\tau^{\pm} \rightarrow 3\pi^{\pm}\nu$ and 960 from $\tau^{\pm} \rightarrow \pi^{\pm}(> 2\gamma)\nu$ to be 0.007 ± 0.002. Using the measured misidentification probability and Monte Carlo simulations, we obtain estimates of these backgrounds. The kinematics of two-photon processes are studied with data and a Monte Carlo based on the double-equivalent photon approximation[7]. Our main two-photon background is from $e^+e^- \rightarrow e^+e^-\mu^+\mu^-$ events. Because existing two-photon Monte Carlo generators do not include internal final-state radiation, we have estimated the $e^+e^- \rightarrow e^+e^-\mu^+\mu^-\gamma$ background directly from the data. To estimate the higher order QED background $e^+e^- \rightarrow \mu^+\mu^-\gamma$ and $e^+e^- \rightarrow \mu^+\mu^-\gamma(\gamma)$ we use a Monte Carlo allowing multiple initial-state and single final-state bremmstrahlung.[14] All Monte Carlo events include a full simulation of the Mark II dectector. Events are corrected to account for small inaccuracies in detector simulation and event reconstruction. For example, we reject Monte Carlo candidate events where the tagging photon shower lies closer than 1.9° to the muon direction, causing an estimated .8% loss in $\tau \rightarrow \mu\gamma\nu\bar{\nu}$ events and a neglible loss in the other event samples.

The reconstructed mass of the μ-γ candidate is a very useful distribution for comparing observed events with QED calculations. Each of the predicted event samples has a unique mass spectrum, allowing extraction of the branching ratio, $B(\tau \rightarrow \mu\gamma\nu\bar{\nu})$. The mass spectrum is fitted with a maximum likelihood technique to determine the contributions from the six sources considered in this analysis, listed in Table 1. In the fit, the contribution from radiative τ decay is allowed to vary freely, but the contributions from the other sources(j) are constrained to lie near their predicted values(the ratio of fitted-to-expected contribution $f_j^b = 1$) under the assumption of Gaussian error distributions on those predictions. The likelihood function is defined by

$$L \equiv \left[\prod_j \frac{1}{\sqrt{2\pi}\sigma_j^b} e^{-(f_j^b-1)^2/2\sigma_j^{b\,2}}\right] \times \left[\prod_i \frac{x_i^{n_i} e^{-x_i}}{n_i!}\right]$$

where n_i is the number of data points observed in mass bin i, x_i is the total expected number of events in each bin, and σ_j^b is the fractional systematic error on background j, which is estimated to yield N_{ji} events in bin i:

$$x_i \equiv 2N_{\tau\tau}B(\tau \to \mu\gamma\bar{\nu}\nu)\, \epsilon_i^{det} + \sum_j f_j^b N_{ji}$$

where the binned detection efficiency for $\tau \to \mu\gamma\nu\bar{\nu}$ events is ϵ_i^{det}, and $N_{\tau\tau}$ is the total number of expected tau events for an integrated luminosity[15] of $207.9 \pm 0.5 \pm 2.8$ pb^{-1} and a total cross section, $\sigma(e^+e^- \to \tau^+\tau^-(\gamma))$, of .135nb. The fit yields the branching ratio B($\tau \to \mu\gamma\nu\bar{\nu}$) and the factors f_j^b's. The expected mass spectra from the four dominant backgrounds are plotted in Figure 1. The systematic errors σ_j^b arise mostly from the statistics of the data and Monte Carlo samples used to estimate the backgrounds and from uncertainties in branching ratios and cross sections. Table 1 lists the estimated σ_j^b and final fitted f_j^b values, where we divide B($\tau \to \mu\gamma\nu\bar{\nu}$) by its predicted value. Figure 2 shows the mass spectrum from the data and from the six predicted contributions, normalized using the fit procedure. In the figure, the mass distribution from the radiative τ decay signal lies mainly below 0.4 GeV/c^2. In this low mass region, there are 14 data events; after subtracting the expected background(Fig. 1), 8.6 ± 3.8 events remain, which is in agreement with the 8.6 ± 3.7 number of signal events predicted by the fit.

Systematic errors on B($\tau \to \mu\gamma\nu\bar{\nu}$) arise from uncertainties in the luminosity measurement(1.4%), in B($\tau \to \mu\nu\bar{\nu}$)(0.8%), in higher order QED μ-pair processes(1.5%), and in the shape of the mass spectrum for two-photon events(0.8%). There are uncertainties due to simulation of clustering in calorimeter track reconstruction and due to uncertainty in the position of one of the muon walls(5.5%). The dominant error is due to uncertainty in the misidentified τ background from decay modes such as $\tau \rightarrow \rho\nu(10.8\%)$.

The result for the ratio of fitted to calculated radiative decay branching ratio is 1.03 ± 0.44, where the error is the quadratic sum of the statistical and systematic errors. From Monte Carlo studies, we estimate that 90% of the radiative decay events passing all event selection criteria arise from decays in which the energy of the photon in the τ rest frame is greater than .037 GeV. From this estimate, we derive the ratio of the measured width $\Gamma(\tau \rightarrow \mu\gamma\nu\bar{\nu}, E_\gamma > .037 \text{ GeV})$ to the total width[1] for $\tau \rightarrow \mu\nu\bar{\nu}$ to be $1.3 \pm 0.6\%$.

To compare radiative τ-pair production rate with expectation, the level of $e^+e^- \rightarrow \tau^+\tau^-\gamma$ events is now allowed to vary freely in the fit. The resulting ratio of fitted-to-expected number of events from the radiative production of a τ that decays to a muon and passes event selection criteria is 0.91 ± 0.22, where we have used 17.8% for the branching ratio $B(\tau \rightarrow \mu\nu\bar{\nu})$. Systematic errors are similar to those described above and are included in the error. Applying the same event cuts, without the requirement of a nearby photon, to $O(\alpha^2)$ Monte Carlo τ pair events(*i.e.*without radiative corrections), we estimate the fraction of radiative to non-radiative events to be $\sim 4.5\%$, of which $\sim 62\%$ are from final-state radiation. Therefore, τ pair production with visible final-state bremsstrahlung is non-negligible, a consideration not taken into account in some previous branching fraction measurements, such as some measurements of the $\tau \rightarrow \pi\nu$ and $\tau \rightarrow \rho\nu$ modes[16]. Other experimental distributions confirm the agreement between the data and predictions. For example, Figure 3 shows the observed photon energy spectrum in comparison with the expected distribution obtained from the fit to the μ-γ mass spectrum.

In summary, we have observed radiative τ decay, $\tau \rightarrow \mu\gamma\nu\bar{\nu}$, in the Mark II data and have measured the ratio of observed to calculated rate to be 1.03 ± 0.44. The ratio of measured-to-predicted number of events from radiative τ production, $e^+e^- \rightarrow \tau^+\tau^-\gamma$, where one of the τ's decay to $\mu\nu\bar{\nu}$ is found to be 0.91 ± 0.22. We have not seen an indication of anomalous behavior in radiative events.

We thank F. Gilman, U. Schneekloth, A. Sirlin, Y.S. Tsai, and B. Ward and several members of the Mark II collaboration at SLC for useful information and discussions. This work benefitted greatly from a previous study on radiative tagging techniques by K. Riles.

REFERENCES

1. W.J. Marciano and A. Sirlin, Phys. Rev. Lett. **61,** 1815 (1988).
2. F. Gilman and S. Rhie, Phys. Rev. **D31,** 1066 (1985).
3. T.N. Truong *et al.*, Phys. Rev. **D30,** 1509 (1984).
4. M.L. Perl, SLAC-PUB-4632 (1988).
5. R. H. Schindler *et al.*, Phys. Rev. **D24,** 78 (1981).
6. J.A. Jaros, *Proceedings of the International Conference on Instrumentation for Colliding Beam Physics*, SLAC-Report-250 (1982).
7. J.R. Smith, Ph.D. thesis, University of California, Davis, RX-1171 (1982).
8. D.Y. Wu, Details may be found in thesis, in preparation.
9. C. Blocker, Ph.D. thesis, University of California, Berkeley, LBL-10801 (1980).
10. S. Jadach and Z. Was, Comp. Phys. Comm. **36,** 191 (1985).
11. D. Stoker *et al.*, Phys. Rev. **D39,** 1811 (1989).
12. See equation 17b. R.E. Behrends, R.J. Finkelstein and A. Sirlin, Physical Review **101,** 866 (1956).
13. S.M. Berman, Physical Review **112,** 267 (1958).
14. S. Jadach *et al.*, KORAL-Z3 LONG WRITE-UP, draft version 3.6, June 1989.
15. D. Karlen, MarkII memo, September 1987. Ph.D. thesis, Stanford University, SLAC-325 (1988).
16. Particle Data Group, Phys. Lett. **204B,** 1 (1988).

TABLE CAPTIONS

Table 1. Input parameters and results from the fit to extract B($\tau \rightarrow \mu\gamma\nu\bar{\nu}$) from the μ-γ mass spectrum. The σ_j^b's are the estimated fractional systematic error for each process and f_j^b's are the ratio of fitted-to-expected contribution.

FIGURE CAPTIONS

Fig. 1 Mass spectrum from four sources, $e^+e^- \rightarrow \tau^+\tau^-\gamma$, misidentified τ's, $e^+e^- \rightarrow e^+e^-\mu^+\mu^-\gamma$, and radiative μ-pairs which are input to the fit. Backgrounds from hadronic events and from spurious electronic noise in the calorimeter are small and not shown.

Fig. 2 Measured and fitted μ-γ mass spectrum from the fit to extract B($\tau \rightarrow \mu\gamma\nu\bar{\nu}$) described in the text.

Fig. 3 Measured photon energy distribution from the selected μ-γ event sample. The sum of the distributions from all predicted sources, normalized using the results of the fit to the μ-γ mass spectrum, is also shown.

Process	Input σ_j^b	Fit Results f_j^b	Fit Results Number of Events
$\tau \to \mu\gamma\nu\bar{\nu}$	–	1.03	10.4
$e^+e^- \to \tau^+\tau^-\gamma$	.07	0.99	40.3
misidentified τ	.35	1.18	10.5
$e^+e^- \to e^+e^-\mu^+\mu^-\gamma$	.45	1.03	3.3
radiative μ-pair	.25	0.99	2.6
hadronic+spurious γ	.35	1.00	0.2

Table 1

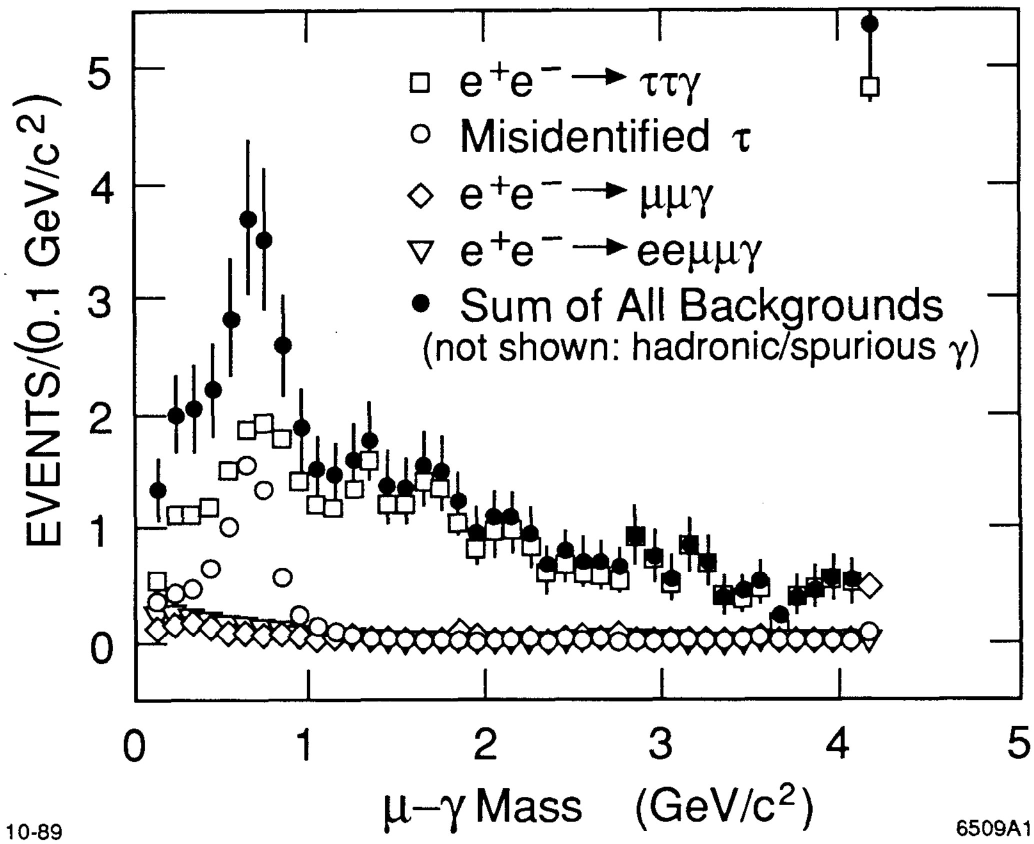

e+e− → ττγ
Misidentified τ
e+e− → μμγ
e+e− → eeμμγ
Sum of All Backgrounds
(not shown: hadronic/spurious γ)
EVENTS/(0.1 GeV/c²)
μ–γ Mass (GeV/c²)
0
1
2
3
4
5
10-89
6509A1

Fig. 1

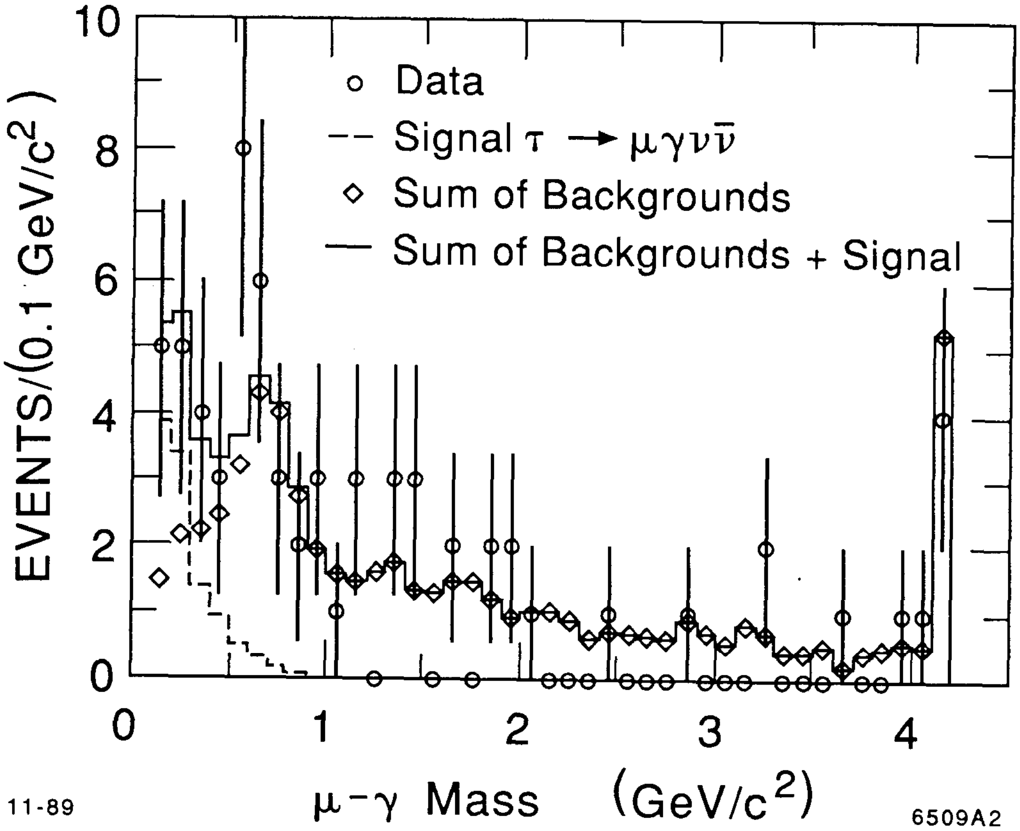
Data
Signal $\tau \rightarrow \mu\gamma\nu\bar{\nu}$
Sum of Backgrounds
Sum of Backgrounds + Signal
EVENTS/(0.1 GeV/c^2)
$\mu-\gamma$ Mass (GeV/c^2)
0
2
4
6
8
10
0
1
2
3
4
11-89
6509A2

Fig. 2

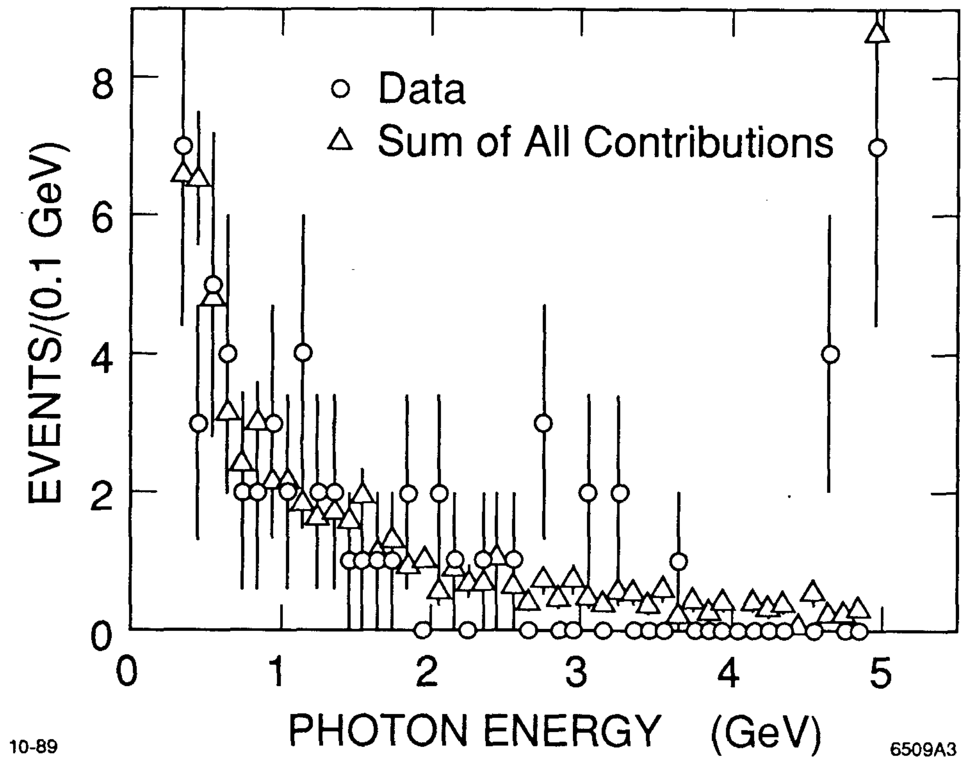

○ Data
△ Sum of All Contributions
EVENTS/(0.1 GeV)
0
2
4
6
8
0
1
2
3
4
5
PHOTON ENERGY (GeV)
10-89
6509A3

Fig. 3